

PAPER • OPEN ACCESS

Fracture response of cement-based composite with spherical glass aggregate exposed to high temperatures

To cite this article: I Rozsypalová *et al* 2019 *IOP Conf. Ser.: Mater. Sci. Eng.* **566** 012027

View the [article online](#) for updates and enhancements.

Fracture response of cement-based composite with spherical glass aggregate exposed to high temperatures

I Rozsypalová¹, I Kumpová^{1,2}, T Majda¹, Z Keršner¹ and P Štancl³

¹ Brno University of Technology, Faculty of Civil Engineering, Veverí 331/95, 602 00 Brno, Czech Republic

² Czech Academy of Sciences, Institute of Theoretical and Applied Mechanics, Centre Telč, Batelovská 485, 486, 588 56 Telč, Czech Republic

³ Statika 3 Structure s.r.o., Designing Company, Nám. ČSA 39, 676 02 Moravské Budějovice, Czech Republic

Abstract. This paper concerns an investigation into the effects of high temperatures acting on specimens made from specially designed fine-grained cement-based composite with spherical glass aggregate. The experimental programme was carried out on four sets of beam specimens with the dimensions $20 \times 40 \times 200$ mm. The specimens were thermally loaded to pre-set temperatures of 100, 200 and 400 °C, after which these temperatures were maintained for 60 minutes (one of the sets contained three reference specimens which were placed in a laboratory at a temperature of 20 °C and were not exposed to heat). After the temperature loading had been performed, the specimens were left to cool down to ambient temperature. After that, fracture tests were used to determine the degree of damage caused to the specimens by temperature loading. Three-point bending tests were conducted on the previously loaded beam specimens, which were notched to provide them with an initial stress concentrator using a diamond blade saw before testing. The depth of the initial edge notch on the bottom side of the specimen was approximately 1/3 of the total specimen depth. The span length was 180 mm. Fracture response was evaluated via load versus deflection diagrams. The monitored parameters were modulus of elasticity, effective fracture toughness and specific fracture energy. Informative compressive strength values were also determined. Selected specimens were investigated using X-ray microtomography (micro-CT).

1. Introduction

Cement-based composites rank amongst those building materials which are frequently used for a wide range of applications [1]. Structures and construction components utilizing this composite are commonly designed assuming normal service temperatures [2]. However, the exposure of cement-based composite to high temperatures causes a wide range of physical and chemical processes to occur within it. These result in changes in the structure of the composite and thus affect its mechanical properties [3–7]. In this paper, the effects of high temperatures acting on specimens made from specially designed fine-grained cement-based composite with spherical glass aggregate are investigated. The monitored parameters were compressive strength, modulus of elasticity, effective fracture toughness, and specific fracture energy. A characterization of the degradation of this cement-based composite when exposed to high temperatures which was gained from data obtained via the ultrasonic pulse method was presented in [8]. In this paper, attention is mainly paid to mechanical fracture properties [9].



Selected specimens were investigated using X-ray micro-tomography (micro-CT) to supplement the results with visual information about the inner structure of the newly designed material before and after thermal loading.

2. Materials and methods

2.1. Specimens

The experimental programme was carried out on four sets of prismatic specimens with the nominal dimensions $20 \times 40 \times 200$ mm. A total of 12 samples were tested. These specimens were formed from fine-grained cement composite. Sodium-potassium glass spheres with a diameter of 2 ± 0.2 mm were used as an aggregate in fresh concrete mixtures. Portland cement (type CEM I 42.5 R – from the Mokra cement plant) was used as a binder. The mix proportion by weight used in this research was 3:1:0.35 aggregate:cement:water.

Specimens (age 28 days) were loaded using a Classic type 5013 laboratory furnace (with 3 sides of heating coils) with a temperature increase of 5 °C/min up to a nominal temperature of 100, 200 or 400 °C. The temperature was then maintained at that level for 60 minutes. One reference set was left without exposure to high temperatures.

2.2. Fracture test

After the temperature loading had been performed, the specimens were left to cool down to ambient temperature. After that, fracture tests were used to determine the degree of damage caused to the specimens by the temperature loading. Three-point bending tests were conducted on the previously loaded beam specimens, which were notched by a diamond blade saw before testing to provide them with an initial stress concentrator – see Figure 1. The depth of the initial edge notch on the bottom side of the specimen was approximately 1/3 of total specimen depth. The span length was 180 mm. Fracture response diagrams – load versus deflection ($L-d$) and load versus crack mouth opening displacement – were measured. The obtained $L-d$ diagrams were corrected and evaluated for this paper via the Effective Crack Model [9] (modulus of elasticity, effective fracture toughness) and Work-of-Fracture Method [10] (specific fracture energy). Informative compressive strength values were determined from fragments of the beams after the fracture tests had been completed [11, 12].

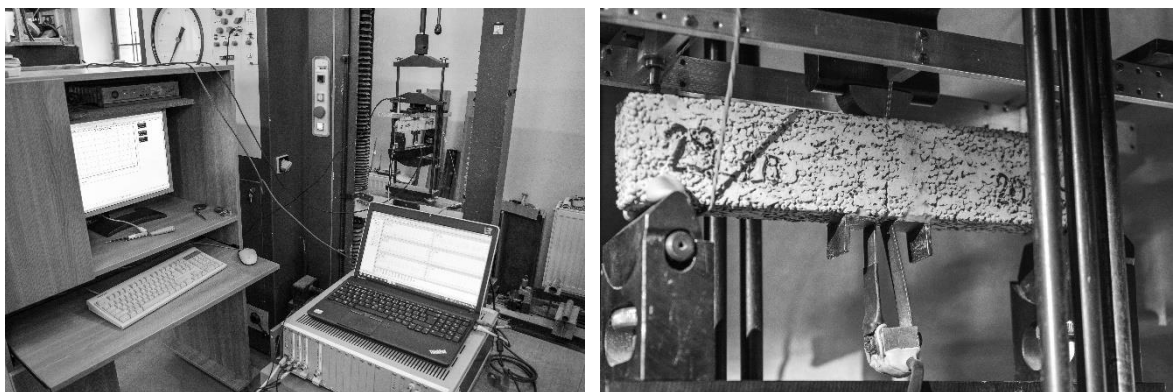


Figure 1. Fracture test configuration in three-point bending: Overall view of the testing machine (left); detail of selected specimen with central edge notch.

2.3. X-Ray micro-tomography

The X-Ray investigation was carried out using the patented TORATOM (Twinned ORthogonal Adjustable Tomograph) device at the Institute of the Theoretical and Applied Mechanics, Centre Telc. The TORATOM system depicted in Figure 2 is a patented (EP2835631) multipurpose X-ray imaging device consisting of two independent pairs of X-ray tube-detectors in an orthogonal arrangement, with a shared rotational stage. All the components are independently adjustable via a multi-axial computer-controlled positioning system, and it is possible to adapt the position of each component according to

the required magnification or resolution and imaging method. The system also allows the observed object to be moved as required, as well as the scanning of objects larger than the detector area.

For qualitative assessment of the degree of damage suffered by the tested fine-grained cement-based composite during exposure to high temperatures, selected specimens were investigated before and after the thermal load using micro-CT. A microfocus X-ray tube (XWT-240-TCHR, X-ray WorX, Germany) operated at a voltage of 160 kV, target current of 281 μ A and a power of 45 W was used for tomographic scanning. A flat panel (Dexela 1512NDT, Perkin Elmer, USA) with an active area of 145.4×114.9 mm, a pixel matrix of 1944×1536 , and a resolution of 74.8 μ m per pixel was used as a detector. The geometric parameters of the tomographic assembly were set in order to obtain the best possible resolution with respect to the object size and the detector area. The source-detector distance was fixed at 600.009 mm and the source-object distance was set to 199.971 mm, resulting in a geometric magnification of the object of about 3.0 \times , leading in the 3D reconstruction to a spatial point edge (voxel) size of 24.933 μ m. CT scans were acquired focusing on the notched part of the specimens. Every CT scan had 600 projections with a 400 ms acquisition time.

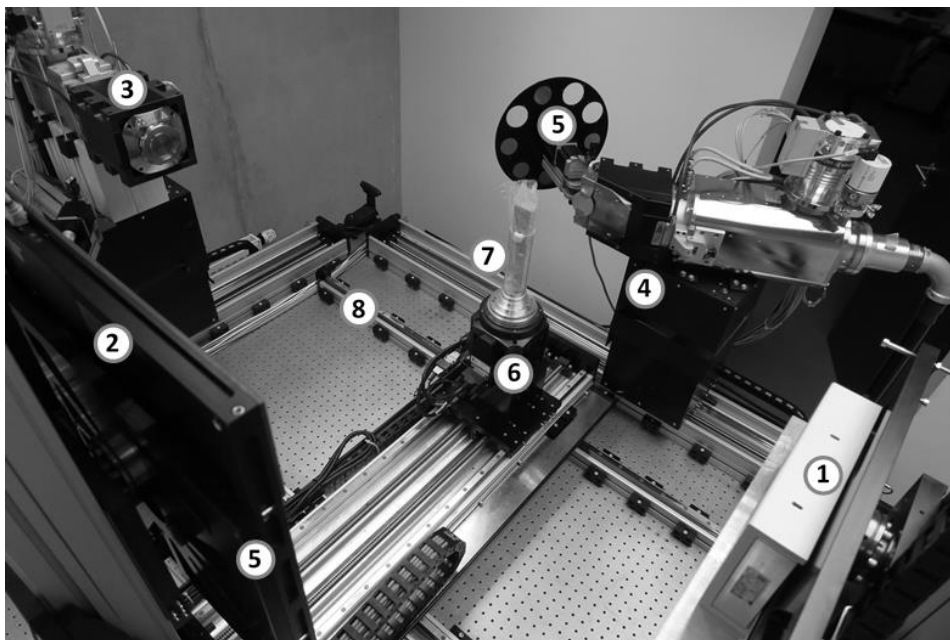


Figure 2. Modular tomographic system TORATOM: 1 – detector holder with large area flat panel detector (145.4×114.9 mm, 74.8 μ m pitch); 2 – detector holder with large area flat panel detector (409.6×409.6 mm, 200 μ m pitch); 3 – nanofocus X-Ray tube (up to 160 kV voltage); 4 – microfocus X-Ray tube (up to 240 kV voltage); 5 – calibration filter holder; 6 – high precision rotary stage; 7 – investigated specimen; 8 – active damped anti-vibration platform with precise CNC positioning system.

3. Results and discussion

The test results can be found in Tables 1–4, which show the values obtained from individual measurements, their arithmetic mean values, standard deviations and coefficients of variation (calculated via functions in Microsoft Excel). For the mean values, relative values are given in parentheses – 100 % always corresponds to the arithmetic mean of the parameter found for specimens without thermal loading (20 °C). Table 5 lists the correlation coefficients (calculated via function in Microsoft Excel) between temperature and mean values for all mechanical fracture parameters.

The compressive strength values (Table 1) gradually decrease with increasing temperature to 40 %. It is possible to notice a very significant drop – at approximately 80–95 % – in the elasticity modulus value (Table 2) for all temperature loaded specimens compared to the reference specimens. A similar situation can also be seen in the case of effective fracture toughness (Table 3) – there is a drop at 90 %

– as well as in the case of specific fracture energy (Table 4) – where there is a decrease at about 80 %. Note that both of these parameter results were obtained with very high variability.

Volumetric images obtained from the CT measurements confirmed that while the structure of the specimen loaded up to 100 °C remains compact, at 200 °C the beginning of disintegration within the interfacial transition zone is observable. At 400 °C disintegration is well propagated, leading to loss of material cohesion. Expansion and interconnection of the pores occurs. Examples of these phases of damage are depicted in Figure 3. The findings are in very good agreement with the values gained for the monitored fracture parameters.

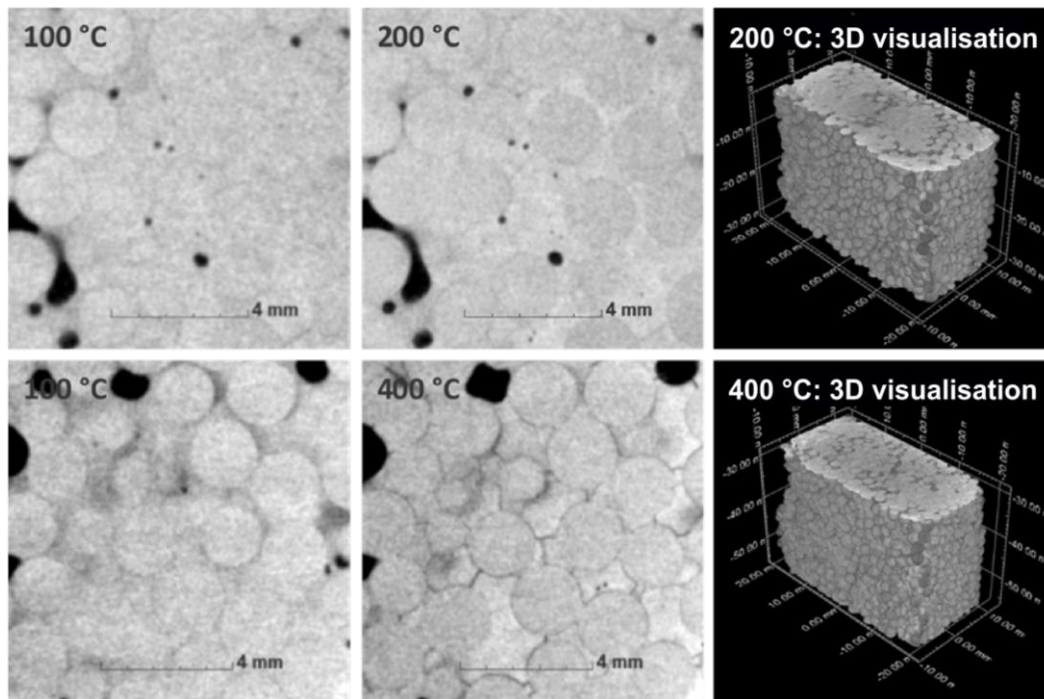


Figure 3. An example of tomographic results. Left – 2D slice visualization of part of a specimen loaded with a temperature of 100 °C; middle – corresponding 2D slice visualisation of part of a specimen loaded with temperatures of 200 °C and 400 °C; right – visualisation of a 3D representation of the volume of interest of a specimen loaded with temperatures of 200 °C and 400 °C.

Table 1. Compressive strength vs. temperature: individual values and basic statistics (relative values).

		Specimen Identification	Value [MPa]	Mean Value [MPa]	Standard Deviation [MPa]	Coefficient of Variation [%]
Maximum Temperature [°C]	20	–	–	11.68	0.07	0.6
		29_20	11.73	(100 %)		
		30_20	11.63			
	100	4_100	8.21	7.56	1.33	17.6
		25_100	6.03	(65 %)		
		27_100	8.44			
	200	6_200	6.91	6.44	1.58	24.5
		7_200	4.68	(55 %)		
		8_200	7.73			
	400	10_400	4.42	4.64	0.50	10.7
		11_400	4.29	(40 %)		
		12_400	5.21			

Table 2. Modulus of elasticity vs. temperature: individual values and basic statistics (relative values).

		Specimen Identification	Value [GPa]	Mean Value [GPa]	Standard Deviation [GPa]	Coefficient of Variation [%]
Maximum Temperature [°C]	20	–	–	23.26 (100 %)	0.53	2.3
		29_20	23.26			
		30_20	22.88			
	100	3_100	4.33	4.30 (18 %)	0.60	14.0
		4_100	3.69			
		25_100	4.89			
	200	6_200	1.13	1.38 (6 %)	0.35	25.3
		8_200	1.63			
		10_400	–			
	400	11_400	4.46	4.41 (19 %)	0.08	1.7
		12_400	4.35			

Table 3. Effective fracture toughness vs. temperature: individual values and basic statistics (relative values).

		Specimen Identification	Value [MPa·m ^{1/2}]	Mean Value [MPa·m ^{1/2}]	Standard Dev. [MPa·m ^{1/2}]	Coefficient of Variation [%]
Maximum Temperature [°C]	20	–	–	0.446 (100 %)	–	–
		29_20	–			
		30_20	0.446			
	100	3_100	0.085	0.110 (25 %)	0.0301	27.3
		4_100	0.102			
		25_100	0.144			
	200	6_200	0.041	0.038 (9 %)	0.0040	10.4
		8_200	0.036			
		10_400	–			
	400	11_400	0.058	0.090 (20 %)	0.0444	49.5
		12_400	0.121			

Table 4. Specific fracture energy vs. temperature: individual values and basic statistics (relative values).

		Specimen Identification	Value [J·m ⁻²]	Mean Value [J·m ⁻²]	Standard Deviation [J·m ⁻²]	Coefficient of Variation [%]
Maximum Temperature [°C]	20	–	–	10.33 (100 %)	–	–
		29_20	–			
		30_20	10.33			
	100	3_100	3.84	5.57 (54 %)	1.79	32.2
		4_100	5.43			
		25_100	7.42			
	200	6_200	3.61	2.30 (22 %)	1.86	80.8
		8_200	0.99			
		10_400	–			
	400	11_400	3.78	6.46 (63 %)	3.79	58.6
		12_400	9.14			

Table 5. Correlation coefficients [–] for temperature and mean values of mechanical fracture parameters.

	T	f_c	E	K_{Ic}	G_F
Maximum Temperature T	1.00				
Compressive Strength f_c	–0.90	1.00		symmetry	
Modulus of Elasticity E	–0.62	0.90	1.00		
Effective Fracture Toughness K_{Ic}	–0.65	0.91	1.00	1.00	
Specific Fracture Energy G_F	–0.39	0.70	0.91	0.91	1.00

4. Conclusion

This work was focused on the evaluation of the degree of damage suffered by fine-grained cement-based composite specimens when exposed to high temperatures. After the exposure of the specimens to elevated temperatures, their mechanical fracture parameters were significantly reduced and their internal structure damaged. The relationship between fracture response and loading temperature for this special cement-based composite with spherical glass aggregate was confirmed: in relation to the increasing temperature, the compressive strength values showed a strong negative correlation, while the modulus of modulus of elasticity and effective fracture toughness values showed a moderate negative correlation and specific fracture energy values showed a weak negative correlation.

5. References

- [1] Aitcin P C and Mindess S 2011 *Sustainability of Concrete* (New York: Spon Press)
- [2] Neville A M 2011 *Properties of Concrete* (Harlow: Pearson Education Limited)
- [3] Bažant Z P and Kaplan M F 1996 *Concrete at High Temperatures: Material Properties and Mathematical Models* (London: Longman Group Limited)
- [4] EN 1991-1-2:2002/AC:2009 *Eurocode 1: Actions on structures – Part 1-2: General actions – Actions on structures exposed to fire*
- [5] Wang Y Burgess I Wald F and Gillie M 2012 *Performance Based Fire Engineering of Structures* (Hoboken: CRC Press)
- [6] Hager I 2013 Behaviour of cement concrete at high temperature *Bull. Pol. Acad. Sci.-Te.* **61** 1–10
- [7] Lim S 2015 *Effects of elevated temperature exposure on cement based composite materials* (Urbana)
- [8] Rozsypalová I Vyhlídal M Dvořák R Majda T Topolář L Pazdera L Šimonová H and Keršner Z 2018 Characterization of cement based composite exposed to high temperatures via ultrasonic pulse method *Acta Polytechnica CTU Proc.* **15** 99–103
- [9] Karihaloo B L 1995 *Fracture Mechanics and Structural Concrete* (New York: Longman Scientific & Technical)
- [10] Rilem Determination of the fracture energy of mortar and concrete by means of three-point bending test on notched beams *Materials and Structures* vol 18 pp 285–290
- [11] ČSN EN 196-1: 2016 *Methods of testing cement – Part 1: Determination of strength*
- [12] BS 1881: Part 119: 1983 *Testing concrete – Part 119 Method for determination of compressive strength using portions of beams broken in flexure (equivalent cube method)*

Acknowledgment

This paper was produced under the “National Sustainability Programme I” project “AdMaS UP – Advanced Materials, Structures and Technologies” (No. LO1408) supported by the Ministry of Education, Youth and Sports of the Czech Republic and Brno University of Technology. The partial financial support of the Czech Science Foundation under project No. 19-01982S is gratefully acknowledged.